The association of MR imaging parameters with pathology of recurrent high grade glioma and treatment-induced effects

J. Cluceru[1,2], S.J. Nelson[1,2], A.M. Molinaro[3], J.J. Phillips[3], M. P. Olson[1], M. LaFontaine[1], A. Jakary[1], D. Nair[1], S. Cha[1], S.M. Chang[3], J.M. Lupo[1]
[1]Dept. Radiology & Biomedical Imaging, [2]Dept. Bioengineering and Therapeutic Sciences, [3]Dept. Neurological Surgery

Overview

MOTIVATION

- Damage induced by chemotherapy and radiation mimics high grade glioma recurrence [1] (Figure 1).
- Radiologists cannot distinguish between these two phenomena and therefore physiologic and metabolic MRI should be used to probe underlying biological difference between treatment induced effects (TxE) and true recurrent high grade glioma (rHGG).
- Distinguishing TxE from rHGG has great implications for treatment planning and clinical trial endpoint evaluation.

THE ROLE OF PHYSIOLOGIC & METABOLIC MRI

- Diffusion weighted imaging (DWI) & diffusion tensor imaging (DTI): ↑ cellularity proliferative tumor potentiates restricted water diffusion, more so than ↑ cellularity from treatment-induced inflammation (Figure 3) [1]; *Parameters used*: ADC = apparent diffusion coeff; FA = fractional anisotropy
- Dynamic susceptibility contrast perfusion-weighted imaging (DSC): Rapid tumor cell division potentiates ↑ angiogenesis and ↑ blood-brain barrier (BBB) breakdown (Figure 4) [4]; *Parameters used:* CBV = cerebral blood volume, PH = deltaR2* peak height, RECOV = percent deltaR2* signal recovery.
- Magnetic resonance spectroscopic imaging (MRSI): Concentrations of metabolites change wrt disease state; use the metabolism of cancer cells to probe differences among TxE and rHGG; *Parameters used:* nCho, nCre, nLac, nLip, nNAA, CNI: Cho-to-NAA index, [2] CCRI: Cho-to-Cre index (Figure 5)

Methods

Patients/Samples: A total of 393 samples from 148 patients with an original diagnosis of high-grade glioma were included in this study. Each patient was recruited prior to resection. The max number of patients were included per analysis (diffusion: 143 pts, 373 samples; perfusion: 132 pts, 232 samples; spectroscopy:
87 pts 187 samples)

Pathology Outcomes: Tumor score (TS) (pathologist evaluation 0-3, 0 = no tumor, 1= <10% tumor, 2 = 10-50% tumor, 3 = >50% tumor); TS 0&1 vs TS 2&3 (grouped); Mib (Ki-67) proliferation marker; TxE vs rHGG (Figure 2); Necrosis (0-2), Treatment-related abnormal blood vessels.

Image Acquisition: Patients were scanned on a 3T GE scanner with an 8-channel head coil. *Anatomic:* T2-weighted FLAIR and FSE as well as T1-weighted pre- and post-gadolinium contrast images. *DTI:* SE EPI images, 24directions, b=1000s/mm^2, 1.7x1.7x3mm resolution *DSC perfusion-weighted imaging*: T2*-weighted EPI images (TR/TE/flip angle = 1250–1500/35–54ms/30–35degrees, 60–80 time points) *3D MRSI:* PRESS volume localization and VSS pulses for lipid signal suppression (TR/TE =1104/144ms, FOV=16×16×16cm^3, nominal voxel size=1×1×1cm^3).

Statistical Analyses:

- Boxplots and histograms were created to observe differences among the distribution of parameters when binned by outcome
- To assess significance in the association of different parameter changes with outcome, Generalized Estimating Equations, Generalized Linear Mixed Models, and repeated measures ANOVA were used to account for the potential correlation among biopsies derived from the same patient.
- GLMM: $\log\left(\frac{P(Y_{ij}=1)}{P(Y_{ij}=0)}\right) = \beta_0 + \beta_1 x_{ij} + bi; i = 1 \ldots ns, j = 1 \ldots m$
- GEE: $\log\left(\frac{P(Y_{ij}=1)}{P(Y_{ij}=0)}\right) = \beta_0 + \beta_1 x_{ij}; i = 1 \ldots n, j = 1 \ldots m$
- These binary methods were extended for ordinal and continuous outcomes using `multgee` and `lme4`, and repeated measures ANOVA, whose model can be written as:
- RM ANOVA: $Yij = \gamma_i + \pi_{ji} + \varepsilon ij; i = 1 \ldots n, j = 1..m$
- All analyses were completed in R statistical computing language

Random Forest experiments:

- Patients were split by patient number into training and testing sets.
- Test set was split again by patient and each sample was then treated as an independent observation for cross validation grid search for best specificity (prediction of TxE or TS = 0)
- Parameters were split by modality and prediction accuracy was tested for each set of parameters (also to avoid complications by missing data)
- Parameters were then combined across modalities to evaluate performance.

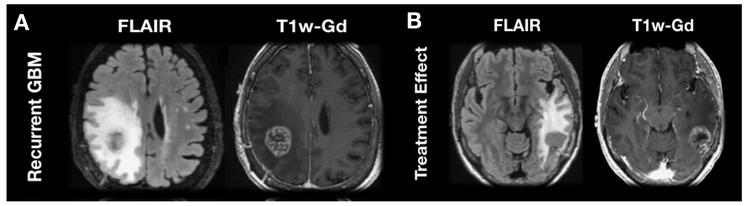

Figure 1. Visual comparison of recurrent HGG and treatment-induced effects. (A) Representative FLAIR and T1w-Gd contrast enhanced (CE) from a recurrent GBM. (B) Representative TMZ and RT induced effects for a suspected recurrent HGG, confirmed TxE from histopathological analysis after resection.

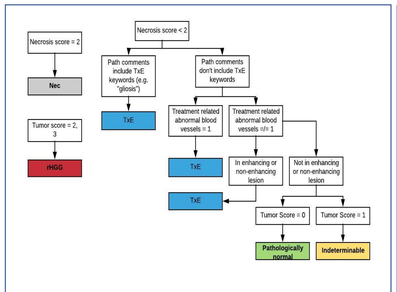

Figure 2. Flow chart depicting the logic for determining categorization of samples into a final TxE pathology. This was necessary due to missing pathological data and no definitive pathological assessment of TxE vs rHGG.

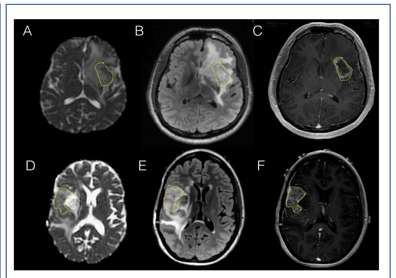

Figure 3. Comparison of ADC images from DTI among treatment effect (A-C) and true recurrent HGG (D-F). Yellow lines delineate T1 contrast enhanced (CE) ROIs. ADC in TxE (A) shows minimal decrease near CE, whereas ADC in rHGG shows significant decrease relative to (A). T2w FLAIR images (B, E) depict hyper-intense regions around the CE from T1. T1w gadolinium injected images (C-F) depict regions of CE.

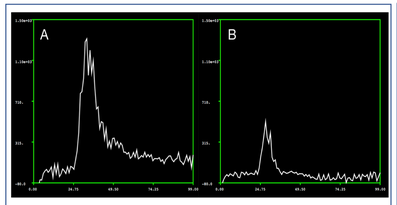

Figure 4. DSC perfusion curve comparison from rHGG vs TxE. Curves representing non-parametric and nonlinear gamma-variate fitting taken from biopsies from (A) pathologically confirmed high-grade glioma and (B) pathologically confirmed treatment effect. Difference in peak height and CBV highlights the utility of DSC imaging in TxE vs. GBM.

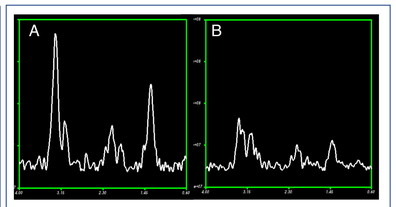

Figure 5. Spectra comparison from rHGG vs TxE. (A) Spectra from a representative voxel taken from a patient experiencing only rHGG. (B) Spectra obtained from a representative voxel from a patient experiencing only Treatment Effect. Spectra shows lowered levels of choline, lactate as compared with (A).

Tables 1 & 2. Patient and sample characteristics.

Pt Demographics		# Pts	% Pts	# Samples	% Samples
Totals		163	100	395	100
Gender	Female (%)	68	41.7	168	42.5
Race	White	134	82.2	321	81.3
	American Indian	1	0.6	2	0.5
	Asian	6	3.7	14	3.5
	Pacific Islander	2	1.2	8	2.1
	Other	20	12.3	44	7.9
WHO	Grade III Astro	12	7.4	31	7.8
	Grade III Oligo	16	9.8	36	9.3
	Grade III Oligoastro	1	0.6	4	1
	Grade IV GBM	102	62.6	246	63
	Grade IV Gliosarc	4	2.5	15	3.7
	Treatment Effect	25	15.3	60	15.2
Age	median, range	52	21-84	n/a	n/a

Sample Chars	Pathscore	# Samples	% Samples
Tumor Score*	0	93	24
	1	53	13.5
	2	115	29.3
	3	131	33.4
Necrosis*†	0	323	80.8
	1	55	13.8
	2	22	5.5
TxE ABV* †	0	84	58.7
	1	59	41.3
TxE or rHGG (Figure 1)**†	TxE	76	23.6
	rHGG	246	76.4

Results

Model Parameters	Spec.	Sens.	Accu-racy	95% CI
nfse, nfl, nt1c, nt1v, nt1d	0.176	0.66	0.42	(0.26, 0.60)
nadc.1, nfa.1, nev1.1, nev2.1, nevrad.1	0.8	0.23	0.54	(0.36, 0.70)
cbvn_nlin, phn_nlin, recov_nlin, phn_npar, recov_npar	0.875	0.5	0.7	(0.50, 0.85)
crni, ccri, cni, nlac, nlip, nLL, nNAA,nCHO, nCRE	0.9	0	0.6667	(0.38, 0.88)

Table 4. Results from multivariate analysis that show predictive performance for preliminary random forest experiments.

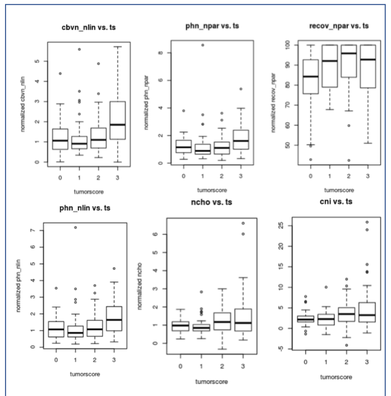

Figure 6. Most visually differentiating parameters. Plotting boxplots of each parameter versus tumor score visually represents differences among imaging parameters when separated by tumor score.

Modality	Parameter	Tumor Score (TS)		TS 0 & 1 vs TS 2 & 3		TxE vs rHGG		Ki-67	
		GEE	GLMM	GEE	GLMM	GEE	GLMM	LMM	RMANOVA
Anatomic	nFSE	n.s.	n.s.	n.s.	n.s.	n.s.	n.s.	n.s.	**
	nFL	n.s.	*	n.s.	*	n.s.	n.s.	n.s.	n.s.
	nT1V	*	*	*	n.s.	*	n.s.	n.s.	**
	nT1C	n.s.	n.s.	n.s.	n.s.	n.s.	n.s.	n.s.	n.s.
Diffusion	nADC	n.s.	n.s.	n.s.	n.s.	n.s.	n.s.	n.s.	*
	nFA	n.s.	n.s.	n.s.	n.s.	n.s.	n.s.	n.s.	*
	nEV1	n.s.	n.s.	n.s.	n.s.	n.s.	n.s.	n.s.	n.s.
	nREV	n.s.	n.s.	n.s.	n.s.	n.s.	n.s.	n.s.	**
Perfusion	nPH_fitted	n.s.	*	*	n.s.	*	n.s.	*	***
	nCBV	*	*	**	*	**	n.s.	***	***
	nPR	*	*	*	n.s.	*	n.s.	n.s.	*
Spectroscopy	nCHO	n.r.	*	*	n.s.	n.s.	n.s.	**	***
	CNI	n.r.	*	**	**	*	n.s.	***	***
	CCRI	n.r.	n.s.	n.s.	n.s.	n.s.	n.s.	**	***
	CRNI	n.r.	n.s.	*	n.s.	n.s.	n.s.	*	*
	nNAA	n.r.	n.s.	n.s.	n.s.	n.s.	n.s.	n.s.	n.s.
	nCRE	n.r.	n.s.	n.s.	n.s.	n.s.	n.s.	n.s.	n.s.
	nLL	n.r.	n.s.	n.s.	n.s.	n.s.	n.s.	n.s.	n.s.

***	p<.001
**	p<.01
*	p<.05

Table 3. Results from univariate analysis that show consistent significance for perfusion and spectroscopy parameters including cerebral blood volume, choline-to-naa index, peak height, and normalized choline.

- Both visual and statistical significance of perfusion and spectroscopy parameters imply associations among imaging characteristics and pathological characteristics.
- Statistical significance is observed for PH, CBV, PR, CNI and CHO in many univariate settings, and multivariate tests imply that the most signal resides in perfusion and spectroscopic techniques as well
- Preliminary investigation into multi-parametric machine learning techniques suggests that there are synergistic properties among parameters that may enable prediction of tumor score

Summary

- Supports literature findings that spectroscopic and perfusion parameters differentiate TxE from rHGG most accurately
- Our results suggest that combining nPH or nCBV from DSC-perfusion with CNI from MRSI hold the most promise in identifying regions of recurrent tumor after treatment.
- Future work will apply a CNN to patient-level data in order to utilize full-patient data.

References

[1] Verma N. et al. *Neuro Oncol* 2013 [2] McKnight TR et al. *J Neurosurg* 2002. [3] Halekoh UJ. et al. *Stat Softw* 2006 [4] Barajas RF et al. *Radiology,* 2009 [5] Jena et al. *American Journal of Neuroradiology,* 2017 [6] Hu LS. et al. *PLoS One* 2015.

Funding: NIH-NCI grant P01 CA118816, NIH T32 Training Grant